

## ORIGINAL ARTICLE

## Lamin B2 prevents chromosome instability by ensuring proper mitotic chromosome segregation

T Kuga<sup>1,2,3</sup>, H Nie<sup>2</sup>, T Kazami<sup>2</sup>, M Satoh<sup>2</sup>, K Matsushita<sup>2</sup>, F Nomura<sup>2</sup>, K Maeshima<sup>4</sup>, Y Nakayama<sup>3</sup> and T Tomonaga<sup>1,2</sup>

The majority of human cancer shows chromosomal instability (CIN). Although the precise mechanism remains largely uncertain, proper progression of mitosis is crucial. B-type lamins were suggested to be components of the spindle matrix of mitotic cells and to be involved in mitotic spindle assembly; thus, B-type lamins may contribute to the maintenance of chromosome integrity. Here, using a proteomic approach, we identified lamin B2 as a novel protein involved in CIN. Lamin B2 expression decreased in colorectal cancer cell lines exhibiting CIN, as compared with colorectal cancer cell lines exhibiting microsatellite instability (MIN), which is mutually exclusive to CIN. Importantly, lamin B2 knockdown in MIN-type colorectal cancer cells induced CIN phenotypes such as aneuploidy, chromosome mis-segregation and aberrant spindle assembly, whereas ectopic expression of lamin B2 in CIN-type colorectal cancer cells prevented their CIN phenotypes. Additionally, immunohistochemical analysis showed a lower expression of lamin B2 in cancer tissues extracted from patients with sporadic colorectal cancer (CIN-type) than that from patients with hereditary non-polyposis colorectal cancer (HNPCC; MIN type). Intriguingly, mitotic lamin B2 in MIN cancer cells was localized outside the spindle poles and mitotic lamin B2 localization was diminished in CIN cancer cells, suggesting an important role of lamin B2 in proper mitotic spindle formation. The obtained results suggest that lamin B2 maintains chromosome integrity by ensuring proper spindle assembly and that its downregulation causes CIN in colorectal cancer.

*Oncogenesis* (2014) 3, e94; doi:10.1038/oncsis.2014.6; published online 17 March 2014

**Subject Categories:** Molecular oncology

**Keywords:** colorectal cancer; chromosomal instability; lamin B2; chromosome segregation; mitotic spindle

## INTRODUCTION

Cancer is widely accepted as a disease of genetic instability. This instability exists as two distinct forms: chromosomal instability (CIN), characterized by gains or losses of whole or large portions of chromosomes, and microsatellite instability (MIN), characterized by mutations at the nucleotide level.<sup>1–3</sup> The fact that most cancers have abnormal chromosomal content, called aneuploidy, indicates that CIN has an important role in carcinogenesis.<sup>4</sup>

CIN has been recognized to occur as a result of chromosome mis-segregation, which is caused by defects in mitotic functions, such as chromosome condensation, sister-chromatid cohesion, kinetochore structure, centrosome formation and microtubule dynamics, as well as the mitotic checkpoint that monitors the proper progression of mitosis.<sup>4</sup> Several proteins involved in mitotic processes have been shown to have mutated or altered expression levels in cancer.<sup>5–8</sup> Moreover, we previously showed that core kinetochore proteins, CENP-A and CENP-H, are overexpressed in colorectal cancer and involved in CIN,<sup>9–11</sup> suggesting that nuclear proteins are also responsible for chromosome integrity.

Nuclear lamins were initially identified as the major components of the nuclear lamina, a proteinaceous layer found at the interface between chromatin and inner nuclear membrane.<sup>12</sup> Although the early view of lamins was as a static nuclear skeleton, recent observations suggest that lamins have far more active roles

throughout the cell cycle, such as DNA replication, transcription and several mitotic events.<sup>13–23</sup> Lamins are grouped as A type (lamins A and C) or B type (lamins B1 and B2) on the basis of their biochemical properties and behavior during mitosis.<sup>24</sup> B-type lamins are expressed in all somatic cell types, whereas A-type lamins are expressed primarily in differentiated cells.<sup>24</sup>

During mitosis, B-type lamin has been observed to associate with the mitotic spindle<sup>25,26</sup> and shown to have an important role in mitotic spindle formation.<sup>14,21</sup> Both depletion and a dominant-negative mutant of lamin B proteins disrupted spindle assembly in mitosis.<sup>21</sup> In *C. elegans*, downregulation of lamin expression induced gross mitotic defects, such as anaphase chromosome 'bridges' and unequal distribution of chromatin to daughter cells.<sup>13</sup> These observations suggest that B-type lamins have an important role in proper chromosome segregation.

In this study, we searched for CIN-related proteins using a proteomic approach and showed the important role of lamin B2 in CIN by manipulating its expression levels in CIN and MIN colorectal cancer cell lines. Moreover, we observed a decreased expression of lamin B2 in human sporadic colorectal cancer tissues (CIN type) as compared with hereditary non-polyposis colorectal cancer tissues (HNPCC, MIN type). Additionally, by dissecting mitotic localization of lamin B2, we suggested a novel mechanism of how lamin B2 maintains mitotic spindle assembly to prevent CIN.

<sup>1</sup>Laboratory of Proteome Research, National Institute of Biomedical Innovation, Osaka, Japan; <sup>2</sup>Department of Molecular Diagnosis (F8), Graduate School of Medicine, Chiba University, Chiba, Japan; <sup>3</sup>Department of Biochemistry and Molecular Biology, Kyoto Pharmaceutical University, Kyoto, Japan and <sup>4</sup>Biological Macromolecules Laboratory, Structural Biology Center, National Institute of Genetics, Shizuoka, Japan. Correspondence: Professor T Tomonaga, Laboratory of Proteome Research, National Institute of Biomedical Innovation, 7-6-8 Saito-Asagi, Ibaraki567-0085, Osaka, Japan.

E-mail: tomonaga@nibio.go.jp

Received 25 May 2013; revised 27 December 2013; accepted 27 January 2014

## RESULTS

Proteomic analysis of colorectal cancer cell lines reveals that lamin B2 is downregulated in CIN cell lines

To search for the factors involved in CIN, we compared protein expression profiles of CIN and MIN colorectal cancer cell lines by a proteomic approach. Both types of cell lines have previously been well studied,<sup>1,27</sup> thus, we used HT29, SW480, SW837 and Caco-2 as CIN cell lines and HCT116, RKO, DLD1 and SW48 as MIN cell lines. Nuclear proteins were extracted from each cell line. Pooled nuclear extracts of CIN cell lines were labeled with Cy5 dyes, whereas those of MIN cell lines were labeled with Cy3 dyes. The labeled proteins were mixed and separated in the same agarose two-dimensional electrophoresis gel (Figure 1a). Proteins that increased or decreased in CIN nuclear extracts (displayed as red or green spots, respectively) were identified by tandem mass spectrometry and their expression levels were validated by western blotting.

One of the clearest differences in expression between CIN and MIN nuclear extracts was that of lamin B2, which significantly decreased in all tested CIN cell lines as compared with MIN cell lines (Figures 1a, arrow and b). In contrast, lamin B1 did not show a clear difference between CIN and MIN cell lines, and the expression of lamin A/C varied between individual cell lines (Figure 1b). Immunofluorescence for lamin B2 further confirmed the decreased level of lamin B2 in CIN cell lines. Although strong lamin B2 staining was detected at the nuclear envelope in several MIN cell lines, the staining was very slight in CIN cell lines (Figure 1c). Thus, these results indicate that the expression of lamin B2 is specifically suppressed in CIN cell lines.

Repression of lamin B2 in MIN cancer cells causes aneuploidy

To examine whether the decreased expression of lamin B2 was involved in CIN, MIN-type HCT116 cells were transfected with lamin B2-siRNA and analyzed for alterations in the chromosome number by fluorescent in situ hybridization (FISH) analysis using several centromere probes (CEPs). Depletion of lamin B2 was checked by western blotting (Figure 2a, lanes 1 and 2) and reverse transcription (RT)-PCR (Supplementary Figure S1). Figure 2b shows that lamin B2 knockdown increased the number of aneuploid cells (arrows). As assessed by counting the number of centromere signals for chromosomes 7, 8, 12 and 15 in at least 200 nuclei, the frequency of aneuploid cells increased 2.2–4.4 times in lamin B2-siRNA-treated cells as compared with control cells (Figure 2c). Similar results were obtained using another lamin B2-siRNA targeting a different region of lamin B2 mRNA (Supplementary Figure S2).

To exclude the possibility that the aneuploidy observed above was due to the off-target effect of lamin B2-siRNA, HCT116 cells were co-transfected with lamin B2-siRNA and lamin B2-GFP plasmid, which would replace the expression and function of endogenous lamin B2. The expression level of lamin B2-GFP was comparable to that of endogenous lamin B2 (Figure 2a). The number of aneuploid cells was then evaluated. By transfection with lamin B2-GFP, the frequency of aneuploidy was markedly decreased as compared with that in cells treated with lamin B2-siRNA alone, and it was almost comparable to that of control-siRNA-treated cells (Figure 2c). These results indicate that the suppression of lamin B2 causes aneuploidy.

To examine the effect of lamin B2 stable knockdown on the proliferation and CIN of cancer cells, we attempted to generate HCT116 MIN cell lines stably depleted of lamin B2 using four plasmids encoding different lamin B2-shRNA. We could obtain only one clone exhibiting ~60–70% depletion of lamin B2 (Supplementary Figure S3a). This clone showed neither increased frequency of aneuploidy (Supplementary Figure S3b) nor alteration in cell proliferation (data not shown). These results suggest that this incomplete depletion of lamin B2 may not be satisfactory to cause CIN, and that a certain level of lamin B2 is sufficient to maintain

chromosome integrity. Because MIN cell lines maintain the checkpoint system against aneuploidy,<sup>28</sup> HCT116 cells depleted of lamin B2 at sufficient levels to cause CIN might be lost by cell death or cell-cycle arrest during the clonal selection. Further study using other approaches is also needed to understand the effects of CIN caused by lamin B2 depletion on cancer survival.

Repression of lamin B2 in MIN cancer cells causes mitotic delay and chromosome mis-segregation

To further examine whether the aneuploidy observed by the depletion of lamin B2 occurred as the result of chromosome mis-segregation, HCT116 cells expressing histone H2B-GFP were treated with lamin B2-siRNA and live-cell imaging of the mitosis was carried out. The duration of mitosis in lamin B2-siRNA-treated cells was significantly longer than in control cells. Compared with control cells that took  $12.5 \pm 5.6$  min from congression to separation of sister chromatids, lamin B2-siRNA-treated cells took more than two times longer ( $28.9 \pm 18.2$  min; Student's *t*-test;  $P = 2 \times 10^{-12}$ ) to complete metaphase (Figure 2d; Supplementary Figure S4; Supplementary Videos 1 and 2). Moreover, lamin B2-depleted cells often showed signs of chromosome mis-segregation, such as chromosome bridges and lagging chromosomes (Figure 2d, arrowheads). These results strongly suggest that lamin B2 is involved in proper chromosome segregation.

Repression of lamin B2 in MIN cancer cells compromises mitotic spindle formation

What is the mechanism of the aberrant mitosis induced by suppression of lamin B2 expression? Recent reports showed that B-type lamins are required for spindle assembly;<sup>14,21</sup> thus, to test the hypothesis that suppression of lamin B2 in MIN cancer cells induces abnormal spindle assembly, two MIN cell lines, HCT116 and RKO, were transfected with lamin B2-siRNA and examined by immunofluorescence with antibodies against  $\alpha$ - and  $\beta$ -tubulin, components of the mitotic spindle. For accumulation of mitotic cells, 48 h after transfection, cells were synchronized with thymidine for 16 h and then cultured in fresh medium for 10–12 h. Depletion of lamin B2 caused a spindle defect or poor spindle morphology with a lack of chromosome congression, whereas control cells showed clear mitotic spindles (Figures 3a and b). Suppression of lamin B2 in HCT116 cells caused an increase in the spindle defect to 40.6% as compared with 16.0% of control cells ( $n = 50$ –100 mitotic cells). These results suggest that depletion of lamin B2 induces mitotic defects, mainly due to aberrant spindle assembly.

Ectopic expression of lamin B2 in CIN cancer cells prevents chromosome mis-segregation and severe aneuploidy

We next examined whether the induction of lamin B2 expression in CIN cancer cells could rescue the mitotic defects characteristic of CIN. CIN-type WiDr cells expressing histone H2B-GFP were transfected with lamin B2-mCherry and live-cell imaging of mitosis was carried out. Expression of lamin B2-mCherry was confirmed by western blotting (Figure 4a) and fluorescence microscopy (Figure 4b). Cells transfected with the control plasmid encoding mCherry alone exhibited chromosome bridges or lagging chromosomes in anaphase at high frequency (38.1%) (Figure 4b; Supplementary Video 3). In addition, these cells showed severe mitotic delay,  $166 \pm 125$  min from nuclear envelope breakdown to anaphase onset (Figure 4c). Strikingly, ectopic expression of lamin B2-mCherry not only decreased the frequency of anaphase chromosome mis-segregation (24.4%) but significantly improved mitotic delay ( $75 \pm 24$  min) (Figures 4b and c; Supplementary Video 4). These results suggest that lamin B2 re-expression promotes accurate chromosome congression and prevents chromosome mis-segregation.

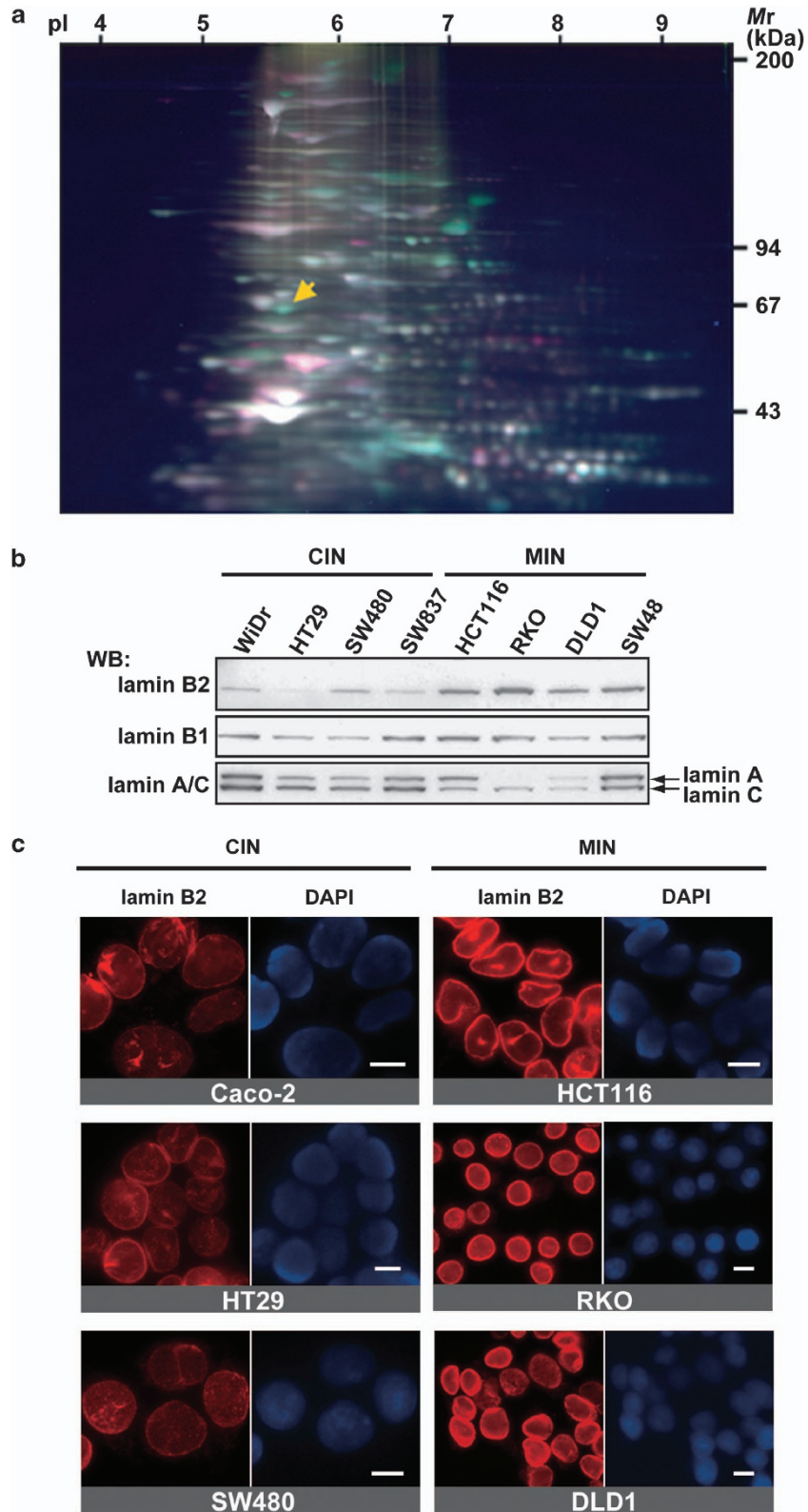


**Figure 1.** Proteomic analysis of colorectal cancer cell lines revealed that lamin B2 is downregulated in CIN cell lines. **(a)** Proteomic analysis of CIN and MIN cell lines using agarose 2D-DIGE. Nuclear extracts prepared from the cell lines were labeled with Cy3 (MIN) and Cy5 (CIN), and separated with two-dimensional electrophoresis. Increased and decreased protein spots in CIN nuclei are displayed as red (Cy5) and green (Cy3), respectively. Yellow arrow shows the protein spot corresponding to lamin B2. **(b)** Western blot analysis of nuclear extracts (10  $\mu$ g) from CIN and MIN cell lines using antibodies to lamin B2, B1 and lamin A/C. **(c)** Immunostaining of CIN and MIN cell lines using anti-lamin B2 antibody and DAPI for DNA. Images show interphase cells. Scale bars, 10  $\mu$ m.

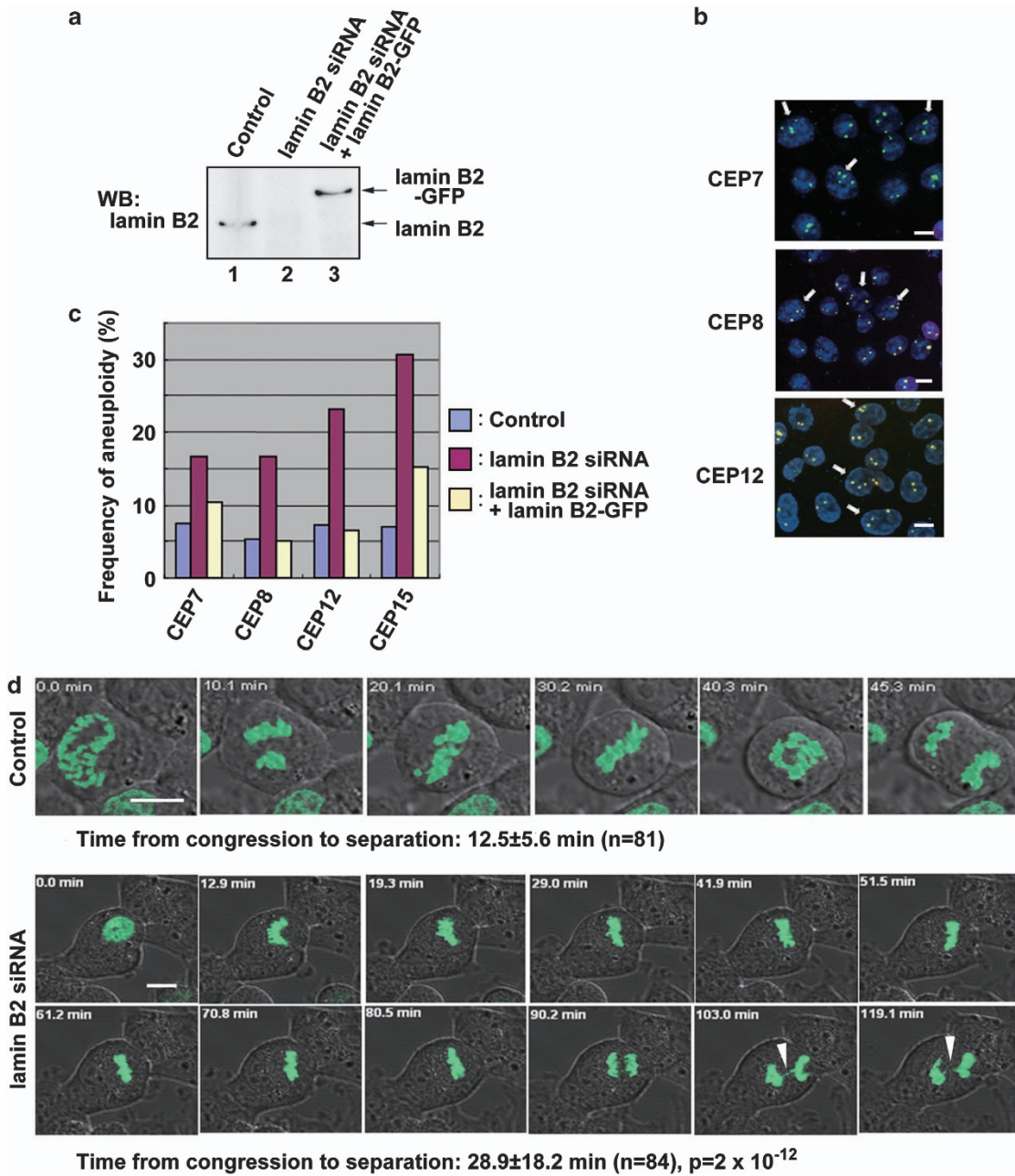


**Figure 2.** Repression of lamin B2 induces mitotic defects and aneuploidy. **(a)** Lamin B2-siRNA alone or together with lamin B2-GFP expression plasmid was transfected into MIN-type HCT116 cells and, 48 h later, the expressions of lamin B2 and lamin B2-GFP were checked by western blotting. Lane 1, control-siRNA; lane 2, lamin B2-siRNA alone; lane 3, lamin B2-siRNA + lamin B2-GFP expression plasmid. **(b)** FISH analysis using centromere probes (CEP7, 8 and 12) was performed 48 h after transfection with lamin B2-siRNA in HCT116 cells. White arrows indicate aneuploid cells. **(c)** Frequency of aneuploid cells in HCT116 cells transfected with either lamin B2-siRNA alone or together with lamin B2-GFP expression plasmid. Centromere singles (CEP7, 8, 12 and 15) were counted in at least 200 cells. **(d)** HCT116 cells stably expressing histone H2B-GFP were treated with control or lamin B2-siRNA for 24 h. Time-lapse images of the cells were taken at 3- to 5-min intervals. Images shown are representative of control or lamin B2-siRNA-treated cells from prophase to anaphase. Control cells took  $12.5 \pm 5.6$  min ( $n=81$ ) from congression to separation of sister chromatids, whereas lamin B2-siRNA-treated cells took  $28.9 \pm 18.2$  min ( $n=84$ ). Arrowheads indicate a chromosomal bridge. Scale bars, 10  $\mu$ m.

We next examined aneuploidy in lamin B2-overexpressed CIN cells. WiDr cells were transfected with lamin B2-GFP or GFP alone (control) and, 7 days after transfection, analyzed by FISH with CEP12 and 15. A large fraction of control cells exhibited three copies of CEP12 and 15 signals, whereas  $9.5 \pm 1.5\%$  and  $14.5 \pm 2.5\%$  of control cells exhibited  $\geq 4$  copies of CEP12 and 15 signals, respectively (Figures 4d and e). Strikingly, ectopic

expression of lamin B2-GFP decreased the number of severely aneuploid cells exhibiting  $\geq 4$  copies of CEP12 ( $6.0 \pm 4.7\%$ ) and CEP15 ( $4.6 \pm 1.5\%$ ) signals, while the number of cells exhibiting 3 copies of these CEP signals increased (Figures 4d and e). Given that intercellular heterogeneity in the chromosome copy number is a typical feature of CIN cancer cells,<sup>1,28</sup> these results suggest that lamin B2 overexpression improves chromosome integrity.

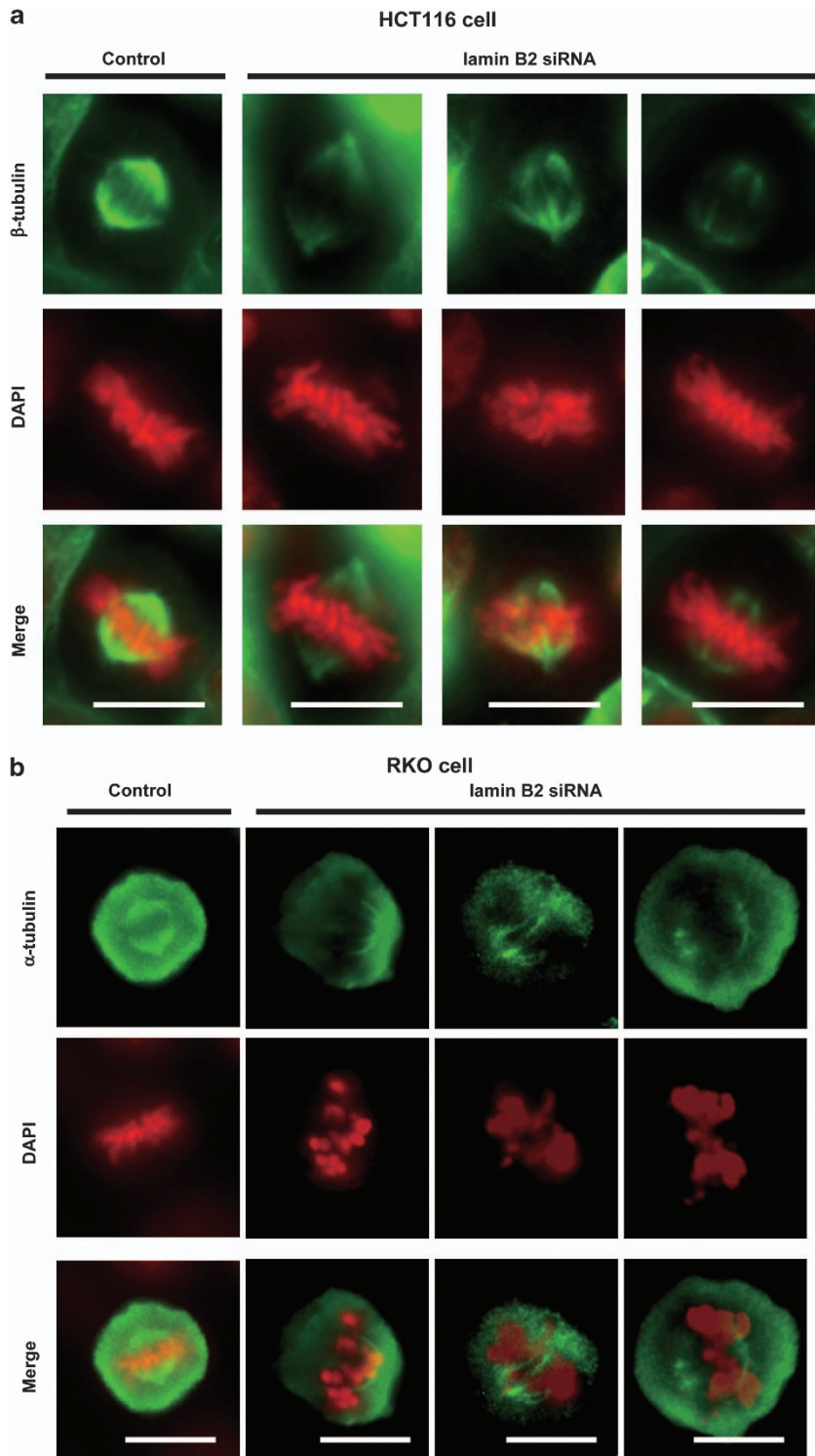


**Figure 3.** Repression of lamin B2 abrogates mitotic spindle formation. MIN cell lines, HCT116 and RKO, were transfected with control- or lamin B2-siRNA. Forty-eight hours after transfection, the cells were synchronized with thymidine for 16 h and then released into fresh medium. Cells that entered mitosis were analyzed by immunostaining using anti- $\beta$ -tubulin (**a**) and  $\alpha$ -tubulin (**b**) antibodies in HCT116 (**a**) and RKO (**b**) cells, respectively. DNA was marked by DAPI. Scale bars, 10  $\mu$ m.

Ectopic expression of lamin B2 in CIN cancer cells prevents aberrant mitotic spindle formation

We further examined mitotic spindle formation in CIN cancer cells with overexpression of lamin B2. To monitor mitotic spindle formation, we generated WiDr cells stably expressing mCherry- $\alpha$ -tubulin.

The cells were transfected with lamin B2-GFP or GFP (control) and live-cell imaging of mitosis was carried out. Control cells showed poor spindle morphology at high frequency (38.0%) during chromosome segregation (Figure 5; Supplementary Video 5), suggesting that mitotic spindle formation is disturbed

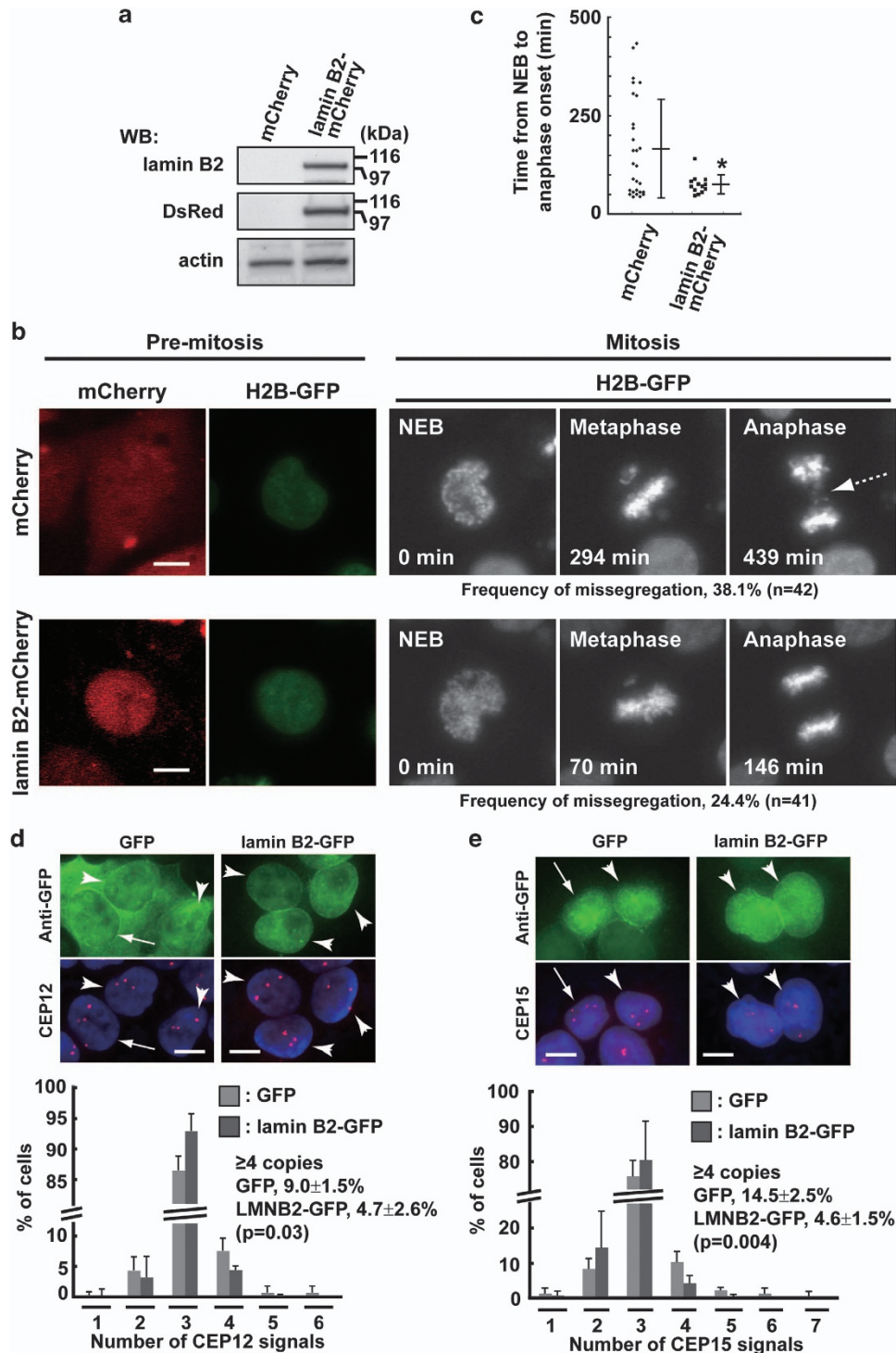


**Figure 4.** Ectopic expression of lamin B2 in CIN cancer cells prevents mitotic defects. (**a–c**) WiDr cells stably expressing histone H2B-GFP were transfected with lamin B2-mCherry or mCherry (control) expression plasmid, and expression of lamin B2-mCherry ( $M_r$ , 96 kDa) was examined by western blotting with anti-lamin B2 and anti-DsRed antibodies (**a**). Anti-DsRed antibody can detect mCherry. Living cells expressing lamin B2-mCherry or mCherry were monitored by confocal microscopy. Representative images of living cells are shown (**b**). Elapsed times from nuclear envelope breakdown (NEB) are indicated at the bottom of mitotic images (**b**). Dotted arrow indicates chromosome mis-segregation in anaphase. Scale bars, 10  $\mu$ m. Percentages of cells exhibiting chromosome mis-segregation during anaphase (mCherry,  $n = 42$ ; lamin B2-mCherry,  $n = 41$ ) are indicated below mitotic images (**b**). (**c**) Plot represents the value of the time from NEB to anaphase onset in each cell, and the means  $\pm$  s.d. are shown (mCherry,  $n = 28$ ; lamin B2-mCherry,  $n = 13$ ). Asterisk indicates a significant difference from the control, calculated by Student's *t*-test ( $*P < 0.05$ ). (**d, e**) CIN-type WiDr cells were transfected with lamin B2-GFP or GFP (control) expression plasmid. Seven days after transfection, cells were analyzed by immunofluorescence with anti-GFP antibody and FISH with CEP12 (**d**) or CEP15 (**e**). DNA was marked by DAPI. Projections of z-stack images at 1- $\mu$ m intervals are shown. Arrowheads and arrows indicate cells exhibiting 3 and  $\geq 4$  copies of CEP signals, respectively. Scale bars, 10  $\mu$ m. Bar diagrams show percentages of cells exhibiting indicated copies of CEP12 (**d**) or CEP15 (**e**) signals. Data are the mean  $\pm$  s.d. of four (**d**) or three (**e**) independent experiments ( $n > 100$  cells for each experiment). The percentage of cells exhibiting  $\geq 4$  copies of CEP12 (**d**) or CEP15 (**e**) signals significantly decreased upon lamin B2 ectopic expression (Student's *t*-test).

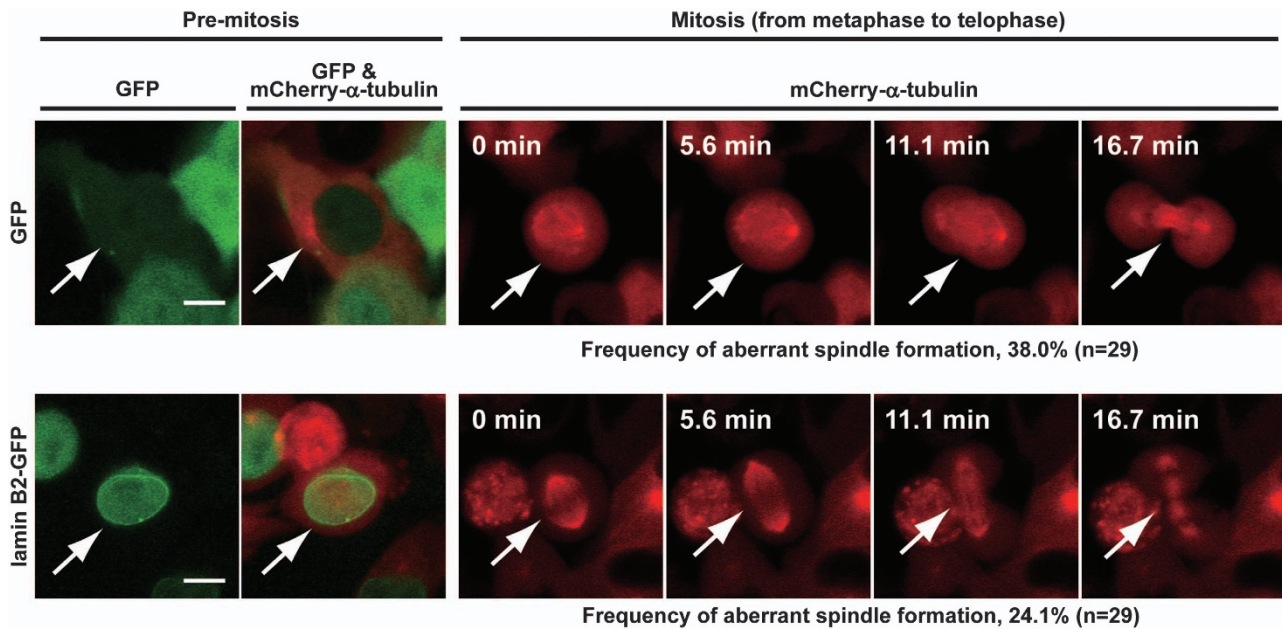


**Figure 5.** Ectopic expression of lamin B2 in CIN cancer cells prevents aberrant mitotic spindle formation. WiDr cells stably expressing mCherry- $\alpha$ -tubulin were transfected with lamin B2-GFP or GFP (control) expression plasmid. Living cells expressing lamin B2-GFP or GFP were monitored by confocal microscopy. Images shown are representative cells (arrows). Scale bars, 10  $\mu$ m. Elapsed times during chromosome segregation are indicated at the top of mitotic images. Percentages of cells exhibiting aberrant spindle formation during mitosis (GFP,  $n = 29$ ; lamin B2-GFP,  $n = 29$ ) are indicated below mitotic images.

in WiDr cells. In lamin B2-GFP-expressing cells, the frequency of poor spindle morphology was reduced (24.1%) (Figure 5; Supplementary Video 6). These results suggest that lamin B2 overexpression improves the accuracy of chromosome segregation by preventing aberrant mitotic spindle formation.

Mitotic lamin B2 localization outside the spindle poles disappears in CIN cancer cells

Previous reports suggested that B-type lamins are structural components of the mitotic spindle matrix required to promote spindle assembly.<sup>21</sup> To visualize mitotic lamin B2 in CIN and MIN cell lines, we performed immunofluorescence with anti-lamin B2 antibody. Although HCT116 and DLD1 MIN lines exhibited intensive staining for mitotic lamin B2 around the spindle poles, SW837 and HT29 CIN lines showed no or very weak staining for mitotic lamin B2 (Figure 6a). These results suggest that CIN cancer cells largely lose the mitotic function of lamin B2.

Unexpectedly, lamin B2 in MIN colorectal cancer cell lines was distributed mainly outside the spindle poles (Figure 6a, magnified images), although the previous report showed co-localization of lamin B2 with kinetochore microtubules in mitotic HeLa cells.<sup>21</sup> Staining of mitotic lamin B2 in HCT116 MIN cells was detected using both rabbit (Figure 6a) and mouse (Figure 6b) anti-lamin B2 antibodies and disappeared upon treatment with lamin B2-siRNA (Figure 6b), confirming the specificity of mitotic lamin B2 staining. Lamin B1 was also localized outside spindle poles, but more broadly than lamin B2. Lamin A/C showed uniform staining throughout the cytoplasm (Figures 6c and d). The specificity of lamins B1 and A/C staining was also confirmed by their knockdown (Figures 6c and d). The mitotic lamin B3 matrix formed in *Xenopus* egg extracts contained spindle assembly factors, including Eg5<sup>21</sup>; however, in HCT116 cells, a large fraction of lamin B2 was not co-localized with Eg5 (Figure 6e). Taken together, these results suggest that the disappearance of mitotic lamin B2 outside the spindle poles is involved in aberrant spindle assembly and chromosome mis-segregation.

SUN1 is a protein associated with mitotic lamin B2

To further understand the role of lamin B2 in spindle formation, we identified proteins associated with lamin B2 in mitosis. Immunoprecipitates using anti-lamin B2, B1 or A/C antibody were prepared from mitotic HCT116 MIN cells and analyzed by LC-MS/MS. By comparing proteins identified from lamin B2 immunoprecipitates with those of lamin B1 and A/C immunoprecipitates, SUN1, an inner nuclear membrane protein,<sup>29,30</sup> was determined as a mitotic lamin B2-associated protein (Supplementary Table S1). In mitotic HCT116 cells, SUN1 was colocalized with lamin B2 and SUN1 staining was attenuated upon knockdown of SUN1 (Figure 6f), indicating that SUN1 is associated with mitotic lamin B2 outside the spindle poles. Since lamins and SUN1 were reported to be involved in stabilizing the position of the nucleus in the cell,<sup>31,32</sup> these results suggest that lamin B2 and SUN1 may contribute to mitotic spindle formation by physically supporting the spindle poles.

Sporadic colorectal cancer tissues (CIN) show decreased lamin B2 expression

The majority of human sporadic colorectal cancer exhibits CIN, whereas HNPCC exhibits MIN.<sup>33</sup> We therefore compared the lamin B2 expression in sporadic colorectal cancer tissues with that in HNPCC tissues. HNPCC patients were diagnosed based on Amsterdam criteria II, and paraffin-embedded tissues from sporadic colorectal cancers and HNPCCs were analyzed by immunohistochemistry with anti-lamin B2 antibody. The staining intensity of lamin B2 is objectively quantified using the TissueFAXS system and the corresponding HistoQuest software (TissueGnostics, Vienna, Austria). Sporadic colorectal cancer tissues showed lower levels of lamin B2 staining than HNPCC (Figures 7a and b; Table 1; Supplementary Figure S5), which supports the idea that repression of lamin B2 is involved in CIN. Interestingly, these data also showed that the mean intensity of lamin B2 expression in HNPCC (MIN) was  $1.3 \pm 0.4$ -fold higher than that in adjacent non-tumor tissues (Student's paired *t*-test,  $P = 0.055$ ). These results suggest not only that a decrease in lamin B2 expression is involved in the induction

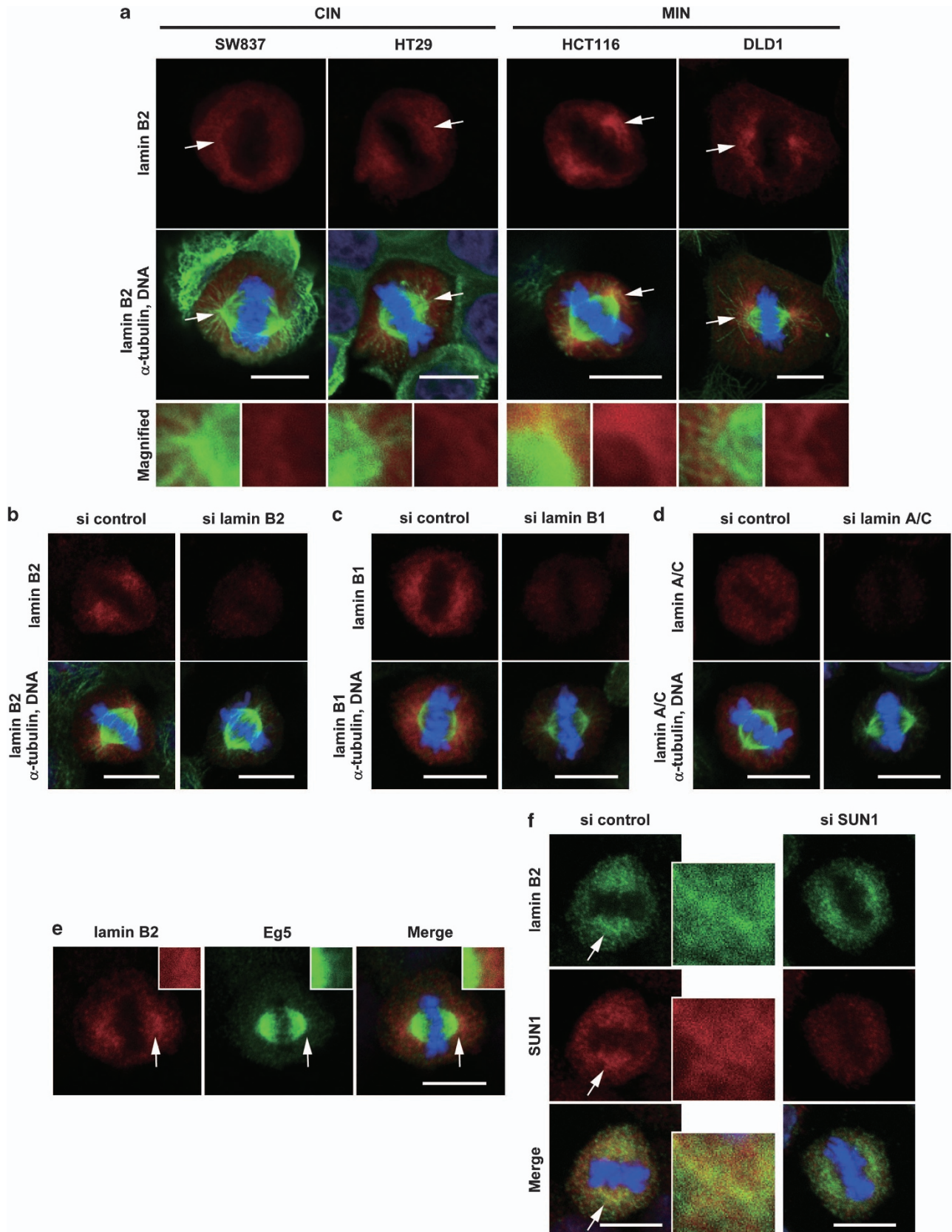


**Figure 6.** Disappearance of immunostaining for mitotic lamin B2 in CIN cell lines. **(a)** CIN (SW837 and HT29) and MIN (HCT116 and DLD1) cell lines were stained with anti-lamin B2 (red) and anti- $\alpha$ -tubulin (green) antibodies. Images show mitotic cells. **(b–d, f)** HCT116 cells were treated with siRNA targeting lamin B2 **(b)**, B1 **(c)** or A/C **(d)** or SUN1 **(f)** and stained with the indicated antibodies. **(e)** HCT116 cells were stained with anti-lamin B2 and anti-Eg5 antibodies. DNA was stained with DAPI (blue). Scale bars, 10  $\mu$ m. The areas indicated by arrows are shown at high magnification.



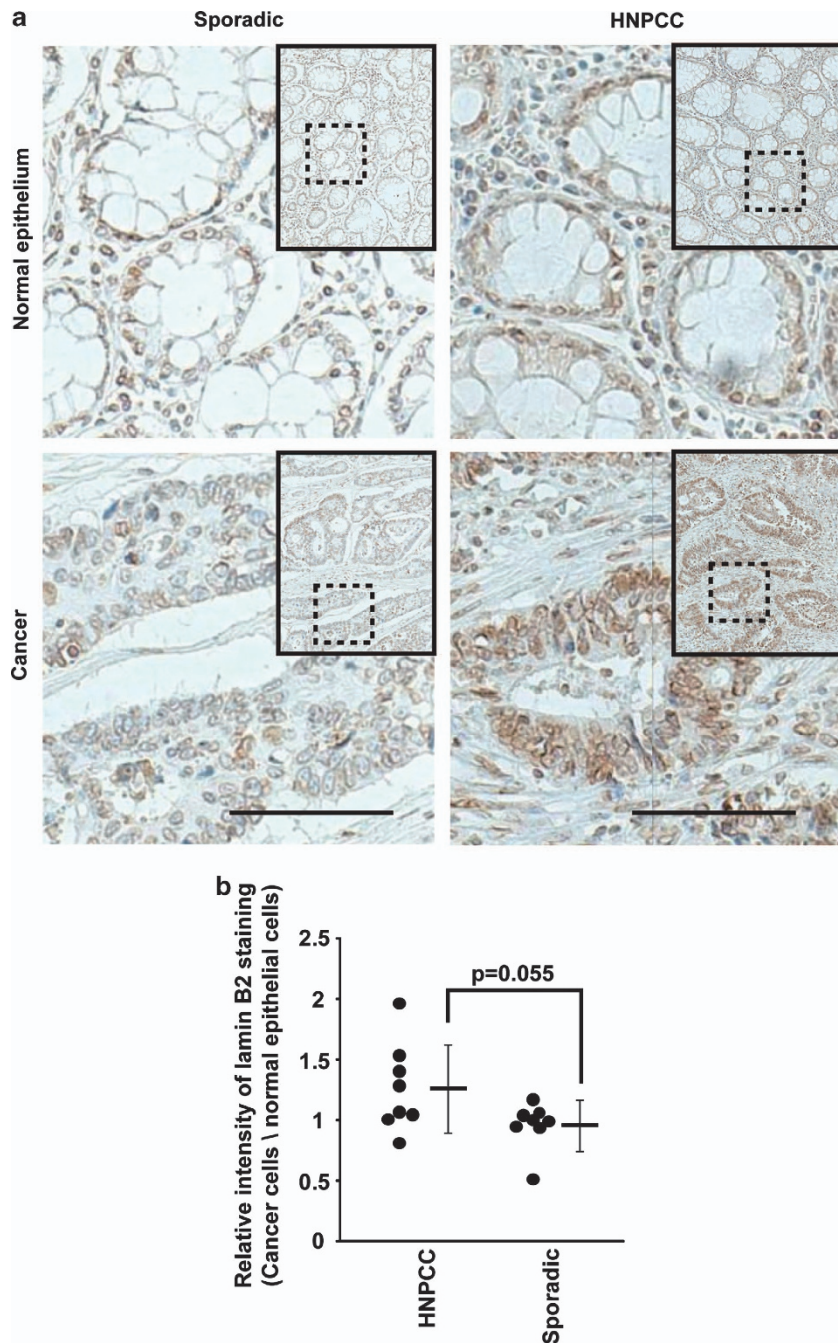


**Figure 7.** Immunohistochemical analysis of lamin B2 in sporadic colorectal cancer and HNPCC. Paraffin-embedded tissue sections of sporadic colorectal cancer (CIN) and HNPCC (MIN) were stained with rabbit polyclonal anti-lamin B2 antibody. Using the TissueFAXS system and HistoQuest software, images of cancer cells and adjacent normal epithelial cells in each tissue section were obtained, and the intensity of lamin B2 staining in these cells was quantitated. (a) Representative images at low and high magnification of the dotted square regions are shown. Bars, 100  $\mu$ m. (b) Plot represents the value of the relative intensity of lamin B2 staining in cancer cells in each tissue section compared with the intensity in adjacent normal epithelial cells in the same tissue section, and the means  $\pm$  s.d. are shown (sporadic colorectal cancer,  $n=8$ ; HNPCC,  $n=8$ ). The  $P$ -value was calculated by Student's  $t$ -test.

of CIN in human colorectal cancer but also that its enhanced expression might be required for MIN cancer to prevent CIN.

## DISCUSSION

In this study, we provided the first evidence that downregulation of lamin B2 is involved in chromosome instability and that restoration of the lamin B2 level is able to prevent mitotic defects. Importantly, low levels of lamin B2 expression were

observed not only in CIN colorectal cancer cell lines but also in sporadic colorectal cancer tissues (CIN). Furthermore, we determined a novel mitotic localization of lamin B2 outside the spindle poles. Our data suggest that lamin B2 has a critical role in preventing CIN in colorectal cancer by maintaining spindle pole stability and consequent spindle assembly.

The major cause of CIN is believed to be chromosome mis-segregation. Proper formation of bipolar spindles is crucial for accurate segregation of chromosomes.<sup>4</sup> Recent studies suggested

**Table 1.** Clinical features of patients with colorectal cancer

	Cancer type	Age	Sex	Location <sup>a</sup>	Histological stage	Lamin B2 level <sup>a</sup>
1	HNPCC	49	Male	R	3	1.4***
2	HNPCC	44	Male	S	4	1.0
3	HNPCC	46	Male	R	1	1.5***
4	HNPCC	44	Male	T	3	2.0***, 1.0 <sup>b</sup>
5	HNPCC	57	Female	A	3	1.3***
6	HNPCC	48	Female	R	3	1.0
7	HNPCC	61	Female	A	2	0.8***
8	Sporadic	67	Male	T	3	0.9*
9	Sporadic	82	Male	A	2	1.2*
10	Sporadic	56	Female	A	3	1.0
11	Sporadic	67	Female	C	3	0.5***
12	Sporadic	41	Female	A	4	0.9
13	Sporadic	60	Male	S	3	1.1
14	Sporadic	67	Male	D,S	4	1.0
15	Sporadic	82	Male	D	2	1.0

Abbreviations: A, ascending colon; C, cecum; D, descending colon; R, rectum; S, sigmoid colon; T, transverse colon. Asterisks indicate significant differences between cancer and normal epithelial cells, calculated by Student's *t*-test (\**P* < 0.05; \*\*\**P* < 0.001). <sup>a</sup>Levels of lamin B2 expression in cancer cells are relative to the adjacent normal epithelial cells (see Supplementary Figure S5). <sup>b</sup>Two distinct tissues from the same patient were examined for lamin B2 expression.

that B-type lamins associate with the mitotic spindle<sup>25,26</sup> and have an active role in mitotic progression by promoting the formation of a spindle matrix.<sup>14,21</sup> Furthermore, downregulation of lamin expression in *C. elegans* induced chromosome mis-segregation.<sup>13</sup> Intriguingly, in CIN colorectal cancer cell lines, lamin B2, but not lamins B1 and A/C, was specifically downregulated (Figure 1). Knockdown experiments of MIN colorectal cancer cells showed that decreased expression of lamin B2 is sufficient to cause aberrant spindle formation, chromosome mis-segregation and aneuploidy (Figures 2 and 3). These results suggest that lamin B2 is a cause of CIN in colorectal cancer.

Mitotic lamin B2 in MIN colorectal cancer cell lines was detected outside spindle poles (Figure 6a), although the previous report suggested that B-type lamins were co-localized with kinetochore microtubules in HeLa cells.<sup>21</sup> Mitotic lamin B2 staining outside the spindle poles was carefully confirmed using two different anti-lamin B2 antibodies and lamin B2 knockdown. The discrepancy might be explained by differences in cell lines or techniques of immunofluorescence.

This study further showed the co-localization of mitotic lamin B2 with an inner nuclear membrane protein SUN1 outside the spindle poles (Figure 6f). SUN1 is known to interact with outer nuclear membrane protein nesprins.<sup>29,34</sup> SUN1 and nesprins bind to lamins and cytoskeletal components, respectively, resulting in nuclear-cytoplasmic connection in interphase cells.<sup>32</sup> In addition, SUN1 was reported to mediate attachment of the nucleus to the centrosome in *C. elegans*.<sup>31</sup> These results indicate that the lamin-SUN1-nesprin complex stabilizes the position of the nucleus in a cell. Intriguingly, nesprin-2 and nesprin-3 were also identified by LC-MS/MS from lamin B2 immunoprecipitates prepared from mitotic HCT116 cells (Supplementary Table S1), suggesting that mitotic lamin B2 makes a complex with SUN1 and nesprins outside the spindle poles. Although the effect of the non-mitotic function of lamin B2 in mitotic processes is unknown, these results imply that the lamin B2 mitotic structure contributes to stabilization of the spindle poles and mitotic spindles.

As CIN is involved in tumorigenesis and tumor progression, prevention of CIN might be an approach for cancer therapy. A number of reports have shown that aberrant expression of mitotic proteins induces chromosome mis-segregation and causes CIN;

however, it is unknown whether most of these proteins actively prevent mitotic defects. Recently, two microtubule-depolymerizing kinesins, Kif2b and MCAK, have been shown to actively prevent chromosome mis-segregation in CIN cancer cell lines.<sup>35</sup> Ectopic expression of these kinesins corrects improper microtubule attachment to kinetochores, leading to protection from chromosome mis-segregation. Our data showed that ectopic expression of lamin B2 in CIN cancer cells rescues aneuploidy and mitotic defects such as chromosome mis-segregation, mitotic delay and aberrant spindle formation (Figures 4 and 5), suggesting that forced expression of lamin B2 seems to promote the correction of chromosome segregation. Given that lamin B2 expression levels are enhanced in HNPCC MIN-type cancer as compared with not only CIN-type cancer but also non-tumor epithelium (Figure 7), enhanced lamin B2 expression in MIN cancer cells might be actively preventing CIN.

Our results may contribute to develop a novel strategy for cancer therapy that specifically targets aneuploid cancer cells. A recent report showed that proliferation of aneuploid, but not euploid, cancer cells is inhibited by AICAR, 17-AAG, chloroquine or their combination.<sup>36</sup> On the other hand, recent meta-analysis identified that MIN tumor patients do not benefit from fluorouracil-based adjuvant chemotherapy.<sup>37</sup> In this respect, determination of the state of chromosome stability of cancer may support a strategy for cancer therapy. Further study is needed to evaluate whether CIN-causative protein lamin B2 is a useful marker for planning a cancer therapy strategy as well as whether ectopic expression of lamin B2 is useful for CIN-preventing therapy.

## MATERIALS AND METHODS

### Cell culture and cell-cycle synchronization

Caco-2, HCT116, SW48, WiDr and RKO colorectal cancer cell lines were purchased from ATCC (Manassas, VA, USA). HT29 and SW480 cell lines and DLD1 and SW837 cell lines were kindly provided by Dr Takenaga and Dr Tagawa (Chiba Cancer Center Research Institute, Chiba, Japan), respectively. Cells were grown at 37 °C in 5% CO<sub>2</sub> in IMDM or RPMI-1640 (Invitrogen, Carlsbad, CA, USA) supplemented with 10% fetal bovine serum (Invitrogen) and 1% penicillin-streptomycin (Invitrogen). To accumulate mitotic cells, cells were pre-synchronized at the G<sub>1</sub>/S phase upon treatment with 2 mM thymidine for 16 h and then released into fresh medium for 10–12 h.

### Plasmid DNA, siRNA and antibodies

To generate lamin B2-GFP and lamin B2-mCherry plasmids, cDNA encoding human lamin B2 was amplified from HeLa cells by PCR using the forward primer 5'-TAAAGCTTATATGGCCACGCCGCTGCC-3' and the reverse primer 5'-ATAGGTACCCACATCAGTAGCAGCCTCTT-3', and was cloned into pEGFP-N1 or pmCherry-N1 vector plasmids (Clontech, Palo Alto, CA, USA). To generate the mCherry- $\alpha$ -tubulin plasmid, full-length human  $\alpha$ -tubulin cDNA was amplified from HeLa cells by PCR using the forward primer 5'-GCAAAGATCTATGCGTGAGTGCATCTCCATCC-3' and the reverse primer 5'-GCGGGGATCCTTAGTATTCTCTCTCTCTTC-3', and was cloned into the pmCherry-C1 vector plasmid (Clontech). The histone H2B-GFP plasmid<sup>38</sup> was kindly provided by Dr Kimura (Kyoto University, Kyoto, Japan). Plasmids encoding lamin B2-shRNA (TRCN0000255440, TRCN0000255441, TRCN0000255443 and TRCN0000255444) or non-target control shRNA (SHC216) were purchased from Sigma-Aldrich (St Louis, MO, USA). Lamin B2-siRNA duplex (TCGGCAATAGCTCACGTTTA) was purchased from Qiagen (Hilden, Germany) and Invitrogen (LMNB2-HSS189214). siRNA duplexes targeting lamins A/C (LMNA-HSS106094) and B1 (LMNB1-HSS106096) were purchased from Invitrogen. siRNA targeting SUN1 (Hs\_UNC84A\_2809) was purchased from Sigma-Aldrich. Control siRNAs were purchased from Qiagen (Firefly luciferase GL2-siRNA) and Invitrogen (Medium GC Duplex#2). Antibodies to the following proteins were purchased: mouse (LN43; Abcam, Cambridge, UK) and rabbit (Proteintech Group, Chicago, IL, USA) anti-lamin B2, goat anti-lamin B1 (sc-6216; Santa Cruz Biotechnology, Santa Cruz, CA, USA), mouse anti-lamin A/C (636; Santa Cruz Biotechnology), mouse (DM1A; Sigma-Aldrich) and rat (YOL1/34; Santa Cruz Biotechnology) anti- $\alpha$ -tubulin, mouse anti- $\beta$ -tubulin

(TUB2.1; Sigma-Aldrich), mouse anti-GFP (Roche, Basel, Switzerland), rabbit anti-DsRed (Clontech), rabbit anti-KIF11 (Eg5) (HPA010568; Sigma-Aldrich), rabbit anti-SUN1 (sc-135077; Santa Cruz Biotechnology), and goat anti-actin (C-11; Santa Cruz Biotechnology) antibodies. Alexa Fluor 488 goat anti-mouse IgG and Alexa Fluor 594 goat anti-mouse IgG antibodies were purchased from Molecular Probes (Eugene, OR, USA). HRP-conjugated anti-mouse IgG (Dako, Glostrup, Denmark), anti-rabbit IgG (GE Healthcare, Little Chalfont, UK) and anti-goat IgG (MP Biomedicals, Santa Ana, CA, USA) antibodies were used.

### Protein extraction and western blotting

Nuclear extracts were obtained from  $\sim 1 \times 10^8$  cells. Cells were resuspended in 5 ml cold buffer (20 mM HEPES-KOH (pH 7.4), 20 mM KCl, 1 mM DTT, 0.1% NP-40, and Complete protease inhibitor cocktail; Roche) and allowed to swell on ice for 15 min. Then, cells were homogenized with a Dounce homogenizer or vigorously vortexed for 15 s 2 times and centrifuged for 5 min at 1000 r.p.m. After pellets were washed twice with the same cold buffer, they were solubilized in lysis buffer (7 M urea, 2 M thiourea, 4% w/v CHAPS, 30 mM Tris-HCl (pH 8.5) and Complete) by passing through 26-gauge needles and were then ultracentrifuged for 1 h at 100 000 g. For extraction of whole-cell proteins, cells were directly lysed in SDS-PAGE sample buffer. Western blotting was performed using the enhanced chemiluminescence (ECL) detection system (GE Healthcare), as described previously.<sup>22,39</sup>

### RT-PCR

Extraction of total RNA and cDNA synthesis were performed as described previously.<sup>40</sup> The expression levels of lamin B2 mRNA were examined by PCR using the forward primer 5'-TCCGCACCGTCCTGGTTA-3' and the reverse primer 5'-CCTGTTGGTGGAAAAGATCCTC-3'. The primer pair for GAPDH (RPP-401) was purchased from TOYOBO (Osaka, Japan).

### Agarose 2D-DIGE and protein identification

Agarose 2D-DIGE was performed as described previously.<sup>41</sup> Pooled nuclear extracts (50  $\mu$ g) of CIN cell lines (HT29, SW480, SW837 and Caco-2) and MIN cell lines (HCT116, RKO, DLD1 and SW48) were labeled with 400 pmol of Cy5 and Cy3, respectively. Internal standard, created by pooling aliquots of all the samples, was labeled with Cy2. The mixed labeled extract (50  $\mu$ g each) was applied to agarose 2D-DIGE. In-gel tryptic digestion of proteins and identification by mass spectrometry were performed as described previously.<sup>41,42</sup>

### Immunoprecipitation-LC-MS/MS

To collect mitotic HCT116 cells, cells were treated with 10  $\mu$ M RO-3306 (Enzo Life Sciences, Farmingdale, NY, USA) for 19 h to arrest the cell cycle at G<sub>2</sub> phase and then cultured in fresh medium without the drug for further 45 min. To prepare cell lysates used for immunoprecipitation (IP lysates), cells were suspended in phosphate-buffered saline containing 1% NP-40, Complete, and phosphatase inhibitor cocktail PhosSTOP (Roche), and then homogenized by sonication. After centrifugation at 100 000 g for 30 min, the supernatant was collected. Immunoprecipitation was performed using anti-lamin B2 (LN43), A/C, or B1 antibody crosslinked to Protein G Dynabeads (Invitrogen) using dimethyl pimelimidate. IP lysates were reacted with antibody-coated Dynabeads for 1 h at 4 °C, and the absorbed proteins were eluted with SDS-PAGE sample buffer free of reducing agents. After reduction with  $\beta$ -mercaptoethanol, immunoprecipitates were resolved by SDS-PAGE and the gel lane was divided into several pieces, and in-gel tryptic digestion of proteins was performed as described previously.<sup>43</sup> The digested peptides were analyzed by LTQ-Orbitrap XL.<sup>44</sup> Protein identification was performed using the MASCOT search engine v2.4 (the UniProtKB/Swiss-Prot database 2012\_6). Database search parameters were the charge of the precursor ion, 2+ and 3+; peptide mass tolerance, 3 p.p.m.; fragment tolerance, 0.6 Da; allowing up to one missed cleavage; fixed modification, carbamidomethylation of cysteine; variable modification, oxidation of methionine. Proteins were identified based on at least two unique peptides. The number of assigned spectra was calculated by the Scaffold 3 software (Proteome Software, Portland, OR, USA) for semiquantitation.

### Immunostaining and FISH of cell lines

For immunostaining, cells were fixed with acetone for 10 min at 4 °C (Figures 1c and 3) or 4% HCHO for 20 min at room temperature (Figures 4d and e)

or 30 °C (Figure 6), and HCHO-fixed cells were permeabilized in phosphate-buffered saline containing 0.5% Triton X-100 on ice. After blocking in phosphate-buffered saline containing 3% bovine serum albumin and 0.1% Tween-20, cells were stained with appropriate antibodies. Immunostained cells were viewed under an LSM710 confocal microscope with the Zen software (Carl Zeiss, Jena, Germany). The objective lenses were EC Plan-NEO FLUAR  $\times 40/1.3$  and Plan APOCHROMAT  $\times 63/1.4$ . FISH was performed as described previously.<sup>9,10</sup> Probes to the pericentromeric regions of chromosome 7, 8, 12 and 15 were purchased from Vysis (Downers Grove, IL, USA). FISH-stained cells were viewed under a Zeiss fluorescent microscope with a  $\times 40/1.3$  or a  $\times 63/1.4$  oil immersion objective and an AxiVision digital imaging system (Carl Zeiss).

### Transient and stable transfection

Transfection with plasmids or siRNA was performed using Lipofectamine 2000 or RNAiMAX (Invitrogen) as described previously.<sup>9,10</sup> For stable transfection, HCT116 or WiDr cells were transfected with histone H2B-GFP, mCherry- $\alpha$ -tubulin, lamin B2-shRNA, or control shRNA expression plasmid containing the neomycin- or puromycin-resistant gene and then selected in medium containing 400  $\mu$ g/ml geneticin (Invitrogen) or 4  $\mu$ g/ml puromycin (StressMarq Biosciences, Victoria, BC, Canada).

### Live-cell imaging

Cells expressing histone H2B-GFP or mCherry- $\alpha$ -tubulin were mounted on a Zeiss LSM510 confocal microscope equipped with a heating stage (37 °C), CO<sub>2</sub> (5%) incubation chamber, and a  $\times 40/1.2$  water immersion or a  $\times 63/1.4$  oil immersion objective (Carl Zeiss). Cells were monitored at 3- or 5-min intervals. To detect the total fluorescence of histone H2B-GFP or mCherry- $\alpha$ -tubulin in a cell, z-stack images from the cell bottom to the cell top were collected and merged into a single plane at each time point during time-lapse experiments.

### Patients and immunohistochemistry

From HNPCC and sporadic colorectal cancer patients, paraffin-embedded blocks of tumor tissues were collected in the Department of Frontier Surgery, Chiba University Hospital. The definition of HNPCC is based on the Amsterdam II criteria.<sup>33,45</sup> The ethics committee of the Graduate School of Medicine, Chiba University approved the protocol. Written informed consent was obtained from each patient before surgery. Four-micrometer sections from paraffin tissues were fixed on slide glasses. Tissues were immunostained as described previously.<sup>46</sup> After deparaffinization and antigen retrieval with microwave irradiation for 5 min in pH 6.0 citric buffer three times, tissues were stained using anti-lamin B2 antibody and En Vision + (Dako). Tissue sections were counterstained with hematoxylin. Using the TissueFAXS system and the corresponding HistoQuest software, stained tissues were viewed and lamin B2 staining was quantitated. Normal epithelial and cancer cells in at least 12 areas in each tissue section were analyzed for the mean intensity of lamin B2 staining, and the average value was calculated.

### CONFLICT OF INTEREST

The authors declare no conflict of interest.

### ACKNOWLEDGEMENTS

We would like to thank Hironori Funabiki for critical reading of this manuscript and Masumi Ishibashi for technical assistance. This work was supported by a Grant-in-Aid for Research on Biological Markers for New Drug Development H20-0005 to TT from the Ministry of Health, Labour and Welfare of Japan and by a Grant-in-Aid 21390354 to TT from the Ministry of Education, Science, Sports and Culture of Japan. This work was supported by a Grant-in-Aid for Research on Biological Markers for New Drug Development H20-0005 to TT from the Ministry of Health, Labour and Welfare of Japan and by a Grant-in-Aid 21390354 to TT from the Ministry of Education, Science, Sports and Culture of Japan.

### REFERENCES

- Lengauer C, Kinzler KW, Vogelstein B. Genetic instability in colorectal cancers. *Nature* 1997; **386**: 623–627.
- Lengauer C, Kinzler KW, Vogelstein B. Genetic instabilities in human cancers. *Nature* 1998; **396**: 643–649.

- 3 Rajagopalan H, Lengauer C. Aneuploidy and cancer. *Nature* 2004; **432**: 338–341.
- 4 Holland AJ, Cleveland DW. Boveri revisited: chromosomal instability, aneuploidy and tumorigenesis. *Nat Rev Mol Cell Biol* 2009; **10**: 478–487.
- 5 Bischoff JR, Anderson L, Zhu Y, Mossie K, Ng L, Souza B et al. A homologue of *Drosophila aurora kinase* is oncogenic and amplified in human colorectal cancers. *EMBO J* 1998; **17**: 3052–3065.
- 6 Kops GJ, Weaver BA, Cleveland DW. On the road to cancer: aneuploidy and the mitotic checkpoint. *Nat Rev Cancer* 2005; **5**: 773–785.
- 7 Yuen KW, Montpetit B, Hieter P. The kinetochore and cancer: what's the connection? *Curr Opin Cell Biol* 2005; **17**: 576–582.
- 8 Zhou H, Kuang J, Zhong L, Kuo WL, Gray JW, Sahin A et al. Tumour amplified kinase STK15/BTAK induces centrosome amplification, aneuploidy and transformation. *Nat Genet* 1998; **20**: 189–193.
- 9 Tomonaga T, Matsushita K, Yamaguchi S, Ohashi T, Shimada H, Ochiai T et al. Overexpression and mistargeting of centromere protein-A in human primary colorectal cancer. *Cancer Res* 2003; **63**: 3511–3516.
- 10 Tomonaga T, Matsushita K, Ishibashi M, Nezu M, Shimada H, Ochiai T et al. Centromere protein H is up-regulated in primary human colorectal cancer and its overexpression induces aneuploidy. *Cancer Res* 2005; **65**: 4683–4689.
- 11 Tomonaga T, Nomura F. Chromosome instability and kinetochore dysfunction. *Histol Histopathol* 2007; **22**: 191–197.
- 12 Fawcett DW. On the occurrence of a fibrous lamina on the inner aspect of the nuclear envelope in certain cells of vertebrates. *Am J Anat* 1966; **119**: 129–145.
- 13 Liu J, Rolef Ben-Shahar T, Riemer D, Treinin M, Spann P, Weber K et al. Essential roles for *Caenorhabditis elegans* lamin gene in nuclear organization, cell cycle progression, and spatial organization of nuclear pore complexes. *Mol Biol Cell* 2000; **11**: 3937–3947.
- 14 Ma L, Tsai M-Y, Wang S, Lu B, Chen R, Yates III JR et al. Requirement for Nudel and dynein for assembly of the lamin B spindle matrix. *Nat Cell Biol* 2009; **11**: 247–256.
- 15 Maeshima K, Yahata K, Sasaki Y, Nakatomi R, Tachibana T, Hashikawa T et al. Cell-cycle-dependent dynamics of nuclear pores: pore-free islands and lamins. *J Cell Sci* 2006; **119**: 4442–4451.
- 16 Shaklai S, Amariglio N, Rechavi G, Simon AJ. Gene silencing at the nuclear periphery. *FEBS J* 2007; **274**: 1383–1392.
- 17 Shimi T, Pfliegerhaer K, Kojima S, Pack CG, Solovei I, Goldman AE et al. The A- and B-type nuclear lamin networks: microdomains involved in chromatin organization and transcription. *Genes Dev* 2008; **22**: 3409–3421.
- 18 Spann TP, Moir RD, Goldman AE, Stick R, Goldman RD. Disruption of nuclear lamin organization alters the distribution of replication factors and inhibits DNA synthesis. *J Cell Biol* 1997; **136**: 1201–1212.
- 19 Spann TP, Goldman AE, Wang C, Huang S, Goldman RD. Alteration of nuclear lamin organization inhibits RNA polymerase II-dependent transcription. *J Cell Biol* 2002; **156**: 603–608.
- 20 Stewart CL, Roux KJ, Burke B. Blurring the boundary: the nuclear envelope extends its reach. *Science* 2007; **318**: 1408–1412.
- 21 Tsai M-Y, Wang S, Heidinger JM, Shumaker DK, Adam SA, Goldman RD et al. A mitotic lamin B matrix induced by RanGTP required for spindle assembly. *Science* 2006; **311**: 1887–1893.
- 22 Kuga T, Nozaki N, Matsushita K, Nomura F, Tomonaga T. Phosphorylation statuses at different residues of lamin B2, B1, and A/C dynamically and independently change throughout the cell cycle. *Exp Cell Res* 2010; **316**: 2301–2312.
- 23 Maeshima K, Iino H, Hihara S, Funakoshi T, Watanabe A, Nishimura M et al. Nuclear pore formation but not nuclear growth is governed by cyclin-dependent kinases (Cdks) during interphase. *Nat Struct Mol Biol* 2010; **17**: 1065–1071.
- 24 Dechat T, Pfliegerhaer K, Sengupta K, Shimi T, Shumaker DK, Solimando L et al. Nuclear lamins: major factors in the structural organization and function of the nucleus and chromatin. *Genes Dev* 2008; **22**: 832–853.
- 25 Georgatos SD, Pырpasopoulou A, Theodoropoulos PA. Nuclear envelope breakdown in mammalian cells involves stepwise lamina disassembly and microtubule-driven deformation of the nuclear membrane. *J Cell Sci* 1997; **110**: 2129–2140.
- 26 Maison C, Pырpasopoulou A, Theodoropoulos PA, Georgatos SD. The inner nuclear membrane protein LAP1 forms a native complex with B-type lamins and partitions with spindle-associated mitotic vesicles. *EMBO J* 1997; **16**: 4839–4850.
- 27 Tsushimi T, Noshima S, Oga A, Esato K, Sasaki K. DNA amplification and chromosomal translocations are accompanied by chromosomal instability: analysis of seven human colon cancer cell lines by comparative genomic hybridization and spectral karyotyping. *Cancer Genet Cytogenet* 2001; **126**: 34–38.
- 28 Thompson SL, Compton DA. Examining the link between chromosomal instability and aneuploidy in human cells. *J Cell Biol* 2008; **180**: 665–672.
- 29 Crisp M, Liu Q, Roux K, Rattner JB, Shanahan C, Burke B et al. Coupling of the nucleus and cytoplasm: role of the LINC complex. *J Cell Biol* 2006; **172**: 41–53.
- 30 Haque F, Lloyd DJ, Smallwood DT, Dent CL, Shanahan CM, Fry AM et al. SUN1 interacts with nuclear lamin A and cytoplasmic nesprins to provide a physical connection between the nuclear lamina and the cytoskeleton. *Mol Cell Biol* 2006; **26**: 3738–3751.
- 31 Malone CJ, Misner L, Le Bot N, Tsai MC, Campbell JM, Ahringer J et al. The *C. elegans* hook protein, ZYG-12, mediates the essential attachment between the centrosome and nucleus. *Cell* 2003; **115**: 825–836.
- 32 Razafsky D, Hodzic D. Bringing KASH under the SUN: the many faces of nucleocytoplasmic connections. *J Cell Biol* 2009; **186**: 461–472.
- 33 Lynch HT, de la Chapelle A. Hereditary colorectal cancer. *New Engl J Med* 2003; **348**: 919–932.
- 34 Stewart-Hutchinson PJ, Hale CM, Wirtz D, Hodzic D. Structural requirements for the assembly of LINC complexes and their function in cellular mechanical stiffness. *Exp Cell Res* 2008; **314**: 1892–1905.
- 35 Bakhour SF, Thompson SL, Manning AL, Compton DA. Genome stability is ensured by temporal control of kinetochore-microtubule dynamics. *Nat Cell Biol* 2009; **11**: 27–35.
- 36 Tang YC, Williams BR, Siegel JJ, Amon A. Identification of aneuploidy-selective antiproliferation compounds. *Cell* 2011; **144**: 499–512.
- 37 Des Guez G, Schischmanoff O, Nicolas P, Perret GY, Morere JF, Uzzan B. Does microsatellite instability predict the efficacy of adjuvant chemotherapy in colorectal cancer? A systematic review with meta-analysis. *Eur J Cancer* 2009; **45**: 1890–1896.
- 38 Kanda T, Sullivan KF, Wahl GM. Histone-GFP fusion protein enables sensitive analysis of chromosome dynamics in living mammalian cells. *Curr Biol* 1998; **8**: 377–385.
- 39 Kuga T, Hoshino M, Nakayama Y, Kasahara K, Ikeda K, Obata Y et al. Role of Src-family kinases in formation of the cortical actin cap at the dorsal cell surface. *Exp Cell Res* 2008; **314**: 2040–2054.
- 40 Kuga T, Kume H, Kawasaki N, Sato M, Adachi J, Shimizu T et al. A novel mechanism of keratin cytoskeleton organization through casein kinase I $\alpha$  and FAM83H in colorectal cancer. *J Cell Sci* 2013; **126**: 4721–4731.
- 41 Nishimori T, Tomonaga T, Matsushita K, Oh-Ishi M, Kodera Y, Maeda T et al. Proteomic analysis of primary esophageal squamous cell carcinoma reveals downregulation of a cell adhesion protein, periplakin. *Proteomics* 2006; **6**: 1011–1018.
- 42 Tomonaga T, Matsushita K, Yamaguchi S, Oh-Ishi M, Kodera Y, Maeda T et al. Identification of altered protein expression and post-translational modifications in primary colorectal cancer by using agarose two-dimensional gel electrophoresis. *Clin Cancer Res* 2004; **10**: 2007–2014.
- 43 Adachi J, Kumar C, Zhang Y, Mann M. In-depth analysis of the adipocyte proteome by mass spectrometry and bioinformatics. *Mol Cell Proteomics* 2007; **6**: 1257–1273.
- 44 Narumi R, Murakami T, Kuga T, Adachi J, Shimizu T, Muraoka S et al. A strategy for large-scale phosphoproteomics and SRM-based validation of human breast cancer tissue samples. *J Proteome Res* 2012; **11**: 5311–5322.
- 45 Vasen HF, Watson P, Mecklin JP, Lynch HT. New clinical criteria for hereditary nonpolyposis colorectal cancer (HNPCC, Lynch syndrome) proposed by the International Collaborative group on HNPCC. *Gastroenterology* 1999; **116**: 1453–1456.
- 46 Seimiya M, Tomonaga T, Matsushita K, Sunaga M, Oh-Ishi M, Kodera Y et al. Identification of novel immunohistochemical tumor markers for primary hepatocellular carcinoma; clathrin heavy chain and formiminotransferase cyclodeaminase. *Hepatology* 2008; **48**: 519–530.



Oncogenesis is an open-access journal published by Nature Publishing Group. This work is licensed under a Creative Commons Attribution-NonCommercial-NoDerivs 3.0 Unported License. To view a copy of this license, visit <http://creativecommons.org/licenses/by-nc-nd/3.0/>

Supplementary Information accompanies this paper on the Oncogenesis website (<http://www.nature.com/oncsis>)